IN VITRO CHANGES IN MITOCHONDRIAL POTENTIAL, AGGRESOME FORMATION AND CASPASE ACTIVITY BY A NOVEL 17-β-ESTRADIOL ANALOGUE IN BREAST ADENOCARCINOMA CELLS

Danielle S. Nkandeu[1], Thandi V. Mqoco[1], Michelle H. Visagie[1], Barend A. Stander[1], Elize Wolmarans[1], Marianne J. Cronje[2], Annie M. Joubert[1]*

[1]*Department of Physiology, University of Pretoria, South Africa*

[2] *Department of Biochemistry, University of Johannesburg, South Africa*

*Corresponding author: A.M. Joubert, Department of Physiology, University of Pretoria, Private Bag X323, Arcadia, Pretoria, 0007, South Africa Tel.: +27 12 3192246; Fax:+ 27 12 321 1679

E-mail address: annie.joubert@up.ac.za

Abstract

2-methoxyestradiol (2ME2), a natural metabolite of estradiol, exerts antiproliferative and antitumor properties *in vitro* and *in vivo*. Due to its low oral bioavailability, several promising analogues of 2ME2 have been developed. In this study, the *in vitro* influence of compound 2-ethyl-3-O-sulphamoyl-estra-1,3,5(10)16-tetraene (C19), a non-commercially available 17-β-estradiol analogue, was tested on the breast adenocarcinoma MCF-7 cell line. The *in vitro* influence of 24 h exposure to 0.18 μM of C19 on MCF-7 cells was evaluated on cell morphology, cell cycle progression, and possible induction of apoptosis and autophagy. Polarization-optical transmitted light differential interference contrast and fluorescence microscopy revealed the presence of cells blocked in metaphase, occurrence of apoptotic bodies and compromised cell density in C19-treated cells. Hallmarks of autophagy namely, an increase in the number of acidic vacuoles and lysosomes were also observed in C19-treated samples. An increase in the number of cells present in the sub-G_1 fraction, as well as a reduction in mitochondrial membrane potential was observed. No significant alterations in

caspase 8 activity were observed. A two-fold increase in aggresome formation was observed in C19-treated cells. C19 induced both apoptosis and autophagy in MCF-7 cells.

Key words: 2-Methoxyestradiol; MCF-7; Autophagy; Apoptosis

Introduction

Worldwide, there are about 7.4 million cancer deaths per year. [1] As the incidence of common cancer types increases at the age of forty, the prevalence of breast cancer per se augments in the late twenties. [2] Risk factors of breast cancer involve the genetic make-up, mammographic density, atypical hyperplasia, radiation and the effect of estrogen which can be divided into endogenous and exogenous estrogen. [2] Lifestyle factors such as diet, alcohol intake and cigarette smoking also influence the incidence of breast cancer development. [2]

2-Methoxyestradiol (2ME2) is an analogue of 17-β-estradiol that is synthesized by the human body. 2ME2 has a strong anticancer activity and induces apoptosis in cancer cells. [3] 2ME2 activates *c-jun* N-terminal-kinase (JNK) (by phosphorylation) as pro-apoptotic signal; it also inactivates (by phosphorylation) the anti-apoptotic (B-cell lymphoma) Bcl-2 family proteins namely Bcl-2 and Bcl-X_L, culminating in apoptosis via the mitochondrial pathway. Furthermore, 2ME2 activates extracellular signal-regulated-kinase (ERK) and p38 mitogen-activated protein kinase (MAPKs) as anti-apoptotic signals. Phosphorylated ERK and p38 MAPKs contribute to the degradation of the pro-apoptotic Bcl-2 family proteins. [3-9] 2ME2 apoptotic actions include the inhibition of the cell cycle progression, changes in mitochondrial membrane potential and the disruption of DNA.

Despite all the benefits of the drug, its bioavailability is low because of rapid degradation due to metabolism. To overcome the disadvantage of its low bioavailability, many estradiol analogues have been synthesized. Stander *et al.* (2011) designed novel 2ME2 derivatives *in silico* by modification of position 2 and the D-ring of 2ME2 in order to create novel estradiol derivatives (Figure 1). Position 3 was replaced by a sulfamate group in the newly designed drug and changes were made at position 2 to increase the antimitotic properties of the new compound. [4] The 2-methoxyestradiol-bis-sulphamate (2-MeOE2bisMATE) analog of 2ME2 is more resistant to metabolism and its increased bioavailability is due to its

sulphamoyl moieties.[12] Improved oral bioavailability is argued to be as a result of the potential of aryl sulphamoyl containing compounds to reversibly bind to carbonic anhydrase II present in blood cells and in turn circumvent first pass liver metabolism.[13]

ENMD-1198, another analogue of 2ME2 is undergoing clinical trials and the D-ring modification appears to improve bioavailability when compared to 2ME2. [10-15] 2-Ethyl-3-O-sulphamoyl-estra-1,3,5(10)16-tetraene (C19) was previously identified as an antimitotic compound and the 16-dehydration found in C19 corresponds with ENMD-1198.[4,14] Therefore, the sulphamoyl moiety as well as the D-ring modifications will improve bioavailability of C19 when compared to 2ME2.

The aim of this study was therefore to investigate the possible anticancer effects of compound 2-ethyl-3-O-sulphamoyl-estra-1,3,5(10)16-tetraene (C19), one of the newly *in silico*-designed drugs, on breast adenocarcinoma MCF-7 cells. The potential anticancer properties were evaluated with regards to cell cycle progression, possible apoptosis and autophagy induction in the human breast adenocarcinoma MCF-7 cell line.
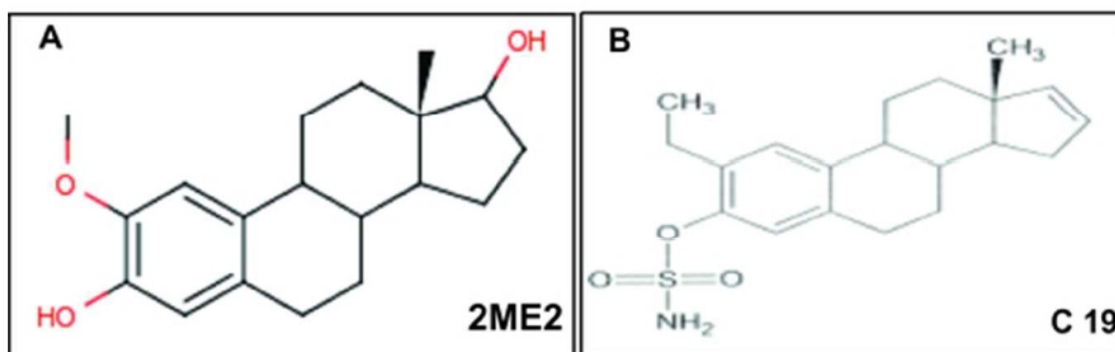

Figure 1. Chemical structures of 2ME2 (A) and compound 2-ethyl-3-O-sulphamoyl-estra-1,3,5 (10)16-tetraene (C19) (B) (drawings by BA Stander using MarvinSketch software available from ChemAxon at http://www. Chemaxon.com/product/marvin_land.html.)

Materials and methods

Materials

Cell line

The MCF-7 (estrogen receptor positive) cell line is a tumorigenic immortalized adherent breast adenocarcinoma cell line that has the ability to chemically transform estradiol via estrogen receptors located in the cytoplasm and can form domes in culture. Cells were purchased from Highveld Biological (Pty) Ltd. (Sandringham, South Africa). MCF-7 cells were cultured in Dulbecco's Minimum Essential Eagle (DMEM) enriched with 10% heat-inactivated FCS, 100 U/mL penicillin G, 100 μg/mL streptomycin, and 250 μg/L fungizone. C19 was dissolved in dimethyl sulfoxide (DMSO) and the final concentration did not exceed 0.05% in cell culture. Cells were exposed to 0.18 μM of C19 for 24 h at 37°C. This concentration was selected since it was previously established that 0.18 μM C19 inhibited cell growth by 50% (GI_{50}) after 24 h at 37°C (Stander *et al*. 2011).

Reagents

All the reagents were obtained from Sigma-Aldrich Co. (St Louis, USA) unless otherwise indicated. Fetal calf serum (FCS) as well as sterile cell culture flasks and plates were supplied by Sterilab Services (Kempton Park, Johannesburg, South Africa). The antibiotics namely penicillin, streptomycin, fungizone and gentamycin were supplied by Highveld Biological (Pty) Ltd (Sandringham, South Africa). Trypsin-EDTA, DMEM and buffers were purchased from Highveld Biological (Pty) Ltd. (Sandringham, South Africa). Actinomycin D served as a positive control for apoptosis, and DMSO served as vehicle control. The caspase 8 colorimetric assay, caspase 7 antibody, the aggresome detection kit, MitoCapture[TM] Mitochondrial Apoptosis Detection Kit and the LC3 antibody were purchased from BIOCOM biotech (Pty) Ltd. (Clubview, South Africa).

Drug synthesis

The compound 2-ethyl-3-O-sulphamoyl-estra-1,3,5(10)16-tetraene (C19) is not commercially available and was *in silico*-designed at the Bioinformatics and Computational Biology Unit, Department of Biochemistry, University of Pretoria, South Africa and synthesized by Ithemba Pharmaceuticals (Pty) Ltd (Modderfontein, Midrand, South Africa).

Cell culture

MCF-7 cells were propagated as monolayers in growth medium at 37°C in a humidified environment containing 5% carbon dioxide. Cells were seeded and allowed for attachment overnight. Appropriate controls were included in all experiments. Cells were propagated in growth medium only; vehicle-treated controls were exposed to 0.6 µL of DMSO in 3 mL DMEM. Cells were exposed to 1.2 µL of tamoxifen in 3 mL DMEM for autophagy detection, as well as cells exposed to 0.3 µL actinomycin D in 3 mL DMEM served as control for apoptosis. Experiments were conducted in 25 cm^2 culture flasks and 6-well plates as stipulated for a specific technique. For 25 cm^2 culture flasks, 10^6 or 500 000 cells were seeded in 3 mL of growth medium. For 6-well plates, 250 000 cells were seeded per well in 3 mL growth medium on heat-sterilized cover slips. For each experiment, growth medium was renewed prior to cell exposure.

Methods

MORPHOLOGY

Triple staining with Acridine orange, Hoechst 33342, and propidium iodide

Fluorescence microscopy was conducted by means of a triple fluorescent staining technique to identify possible intracellular markers of cell death. Acridine orange detects and accumulates in autophagic vacuoles to emit a green fluorescent light. Hoechst 33342 stains the nuclei of apoptotic cells blue, while propidium iodide red fluorescence aggregates in the nuclei of necrotic cells. Cells were seeded at a density of 250 000 cells per well in 6-well plates and allowed to attach overnight. Cells were then exposed to 0.18 µM of C19 and appropriate controls in fresh medium for 24 h. Subsequently 0.5 mL of 0.9 µM Hoechst 33342 and 0.5 mL of 50 µM acridine orange in phosphate saline buffer (PBS) were added to all 6 wells and samples were incubated for 25 min at 37°C. 0.5 mL of 12 µM propidium iodide was added for an additional 5 min. Cells were washed twice with PBS. The experiment was performed in the dark to prevent bleaching. Samples were examined under a Zeiss inverted Axiovert CFL40 microscope and photomicrographs were taken with a Zeiss Axiovert MRm monochrome camera with different fluorescence filters to distinguish between the different stains. Zeiss filter 2 was used for Hoechst 33342 (blue emission), Zeiss

filter 9 for acridine orange (green emission) and Zeiss filter 15 for propidium iodide (red emission) stained cells.

Polarization-optical differential interference contrast

Polarization-optical transmitted light differential interference contrast (PlasDIC) is an enhanced method in which linearly polarized light is emitted after the objective, generating quality images. [5,6] This technique uses a beam of polarized light divided into two beams polarized at 90° to each other; each beam of light takes a slightly different path through the sample [7]. The absorbance of the sample causes the two beams to interfere with each other before they recombine [7]. PlasDIC gives a three-dimensional image of individual cells and cell clusters in plastic cell culture flasks. [5, 6, 7] PlasDIC microscopy was used to non-invasively assess the morphology of the cell population. [7] MCF-7 cells were seeded at a density of 250 000 cells per well in 6-well plates. After an incubation period of 24 h, cells were exposed to 0.18 μM of C19. PlasDIC images were taken using the Zeiss Axiovert-40 microscope (Göttingen, Germany).

Haematoxylin and eosin staining

MCF-7 cells were seeded at a density of 250 000 cells per well in six-well plates on heat-sterilized coverslips. After an incubation period of 24 h at $37^{o}C$ and 5% carbon dioxide, cells were exposed to 0.18 μM C19 and appropriate controls for 24 h at $37^{o}C$ and 5% carbon dioxide. The coverslips were then removed and transferred to a staining dish. Cells were fixed in Bouin's fixative for 30 min. The fixative was discarded and 70% ethanol was added to the coverslips for 20 min. The coverslips were rinsed with tap water for 2 min and stained with haematoxylin for 20 min. After rinsing with tap water for 2 min, coverslips were washed with 70% ethanol and stained with eosin for 7 min. The coverslips were dehydrated in a stepwise manner using 70% ethanol twice for 5 min, 96% ethanol twice for 5 min and 100% ethanol twice for 5 min and xylol for 5 min after which they were mounted on microscope slides using resin to allow for permanent attachment of the cells onto the slides and left to dry overnight. The sample was evaluated using a Zeiss inverted Axiovert CFL40 microscope and photomicrophaghs were taken using a Zeiss Axiovert MRm monochrome camera (Carl Zeiss MicroImaging, Inc.,New York, USA). Mitotic indices were obtained by counting 1000 cells per slide and expressing it as a percentage of cells in mitosis and apoptosis.

SPECTROPHOTOMETRY

Caspase 8 activation assay

The activation of caspase 8 (an initiator caspase of apoptosis) was determined using a FLICE/Caspase 8 colorimetric kit. MCF-7 cells were seeded at a density of 10^6 cells per 25 cm^2 flask. Cells were incubated for 24 h to allow for attachment, the medium was discarded and the cells were exposed to 0.18 μM C19, DMSO and actinomycin D respectively. Cells were trypsinized and centrifuged at 10.000 × g. Cells were resuspended in 50 μL of chilled cell lysis buffer and incubated on ice for 10 min. Cells were centrifuged at 10.000 × g for one min. The supernatant was transferred to a new tube and left on ice for 15 min. After the protein concentration was determined using a standard curve, 100 μg protein /50 μL cell lysis buffer was mixed with 50 μL reaction buffer containing 10 mM of DTT. 5μL of 4 mM VEID-pNA substrate with a final concentration of 200 μM was added to the mixture and incubated at 37°C for 2 h. Absorbances were read at 405 nm using the EL$_x$800 Universal Microplate Reader purchased from Bio-Tek Instruments Inc., (Vermont, USA).

FLOW CYTOMETRY

Caspase 7 activation assay

The activation of caspase 7 (an effector caspase of apoptosis) was determined using a FITC Caspase 7 kit. MCF-7 cells were seeded at a density of 10^6 cells per 25 cm^2 flask. After 24 h attachment the medium was discarded and cells were exposed to 0.18 μM C19, DMSO and actinomycin D. Cells were trypsinized and centrifuged at 10.000 × g. Cells were washed with 0.5 mL PBS, were centrifuged then the supernatant was discarded. 0.5 mL fixation buffer was added and the samples were incubated at room temperature for 20 min. After the supernatant was discarded, the cell suspension was resuspended in 0.5 mL PBS. After the supernatant was centrifuged and discarded, cell suspension was resuspended in 0.5 mL ice-cold cell lysis buffer containing 0.5% Tween 20 and incubated at 4°C for 20 min. After another centrifugation step, 0.5 mL 1 × assay buffer was added to the cell suspension. The supernatant was discarded and 100 μL 1 × assay buffer was added followed by 100 μL primary antibody cocktail. The cell samples were incubated at 4°C for 90 min. 900 μL of 1 × assay buffer was added, centrifuged and the supernatant was discarded. 100 μL of 1 × assay buffer was added as well as 100 μL of secondary antibody

cocktail. The samples were protected from light to avoid bleaching. Samples were incubated at 4°C for 60 min. The samples were then centrifuged and the supernatant was discarded. Samples were washed twice using 0.5 mL 1 × assay buffer and were analysed using flow cytometry. Data from at least 10 000 cells were analyzed by means of Cyflogic version 1.2.1 software (Pertu Therho, Turko, Finland).

FLOW CYTOMETRY

Cell cycle progression

Influences on cell cycle progression and mitochondrial membrane potential were investigated by means of flow cytometry. Cells were seeded at a density of 10^6 cells per 25 cm^2 flask and were incubated overnight to allow for attachment. Cells were subsequently exposed to 0.18 μM of C19 for 24 h and appropriate controls were included as previously described. Cells were trypsinized and washed in 1 mL PBS. After centrifugation, the cells were resuspended in 200 μL ice-cold PBS containing 0.1% fetal bovine serum. Cells were fixed in 4 mL of ice-cold 70% ethanol and the samples were kept overnight at 4°C. Cells were washed and re-suspended in 1 mL of PBS containing propidium iodide (40 μg/mL), RNAse A (100 μg/mL) and Triton X-100 (0.1%) for 40 min at 37°C. Analyses were performed using a Beckman Coulter Cytomics FC500 instrument (Beckman Coulter Inc., Fullerton, CA, USA). Data from at least 30 000 cells per sample were analyzed by means of CXP software (Beckman Coulter (Pty) Ltd, South Africa. Data from cell debris and aggregated cells were removed. For cell cycle progression, results were expressed as percentage of these cells in each phase. Collected data were analyzed using Cyflogic software (Cyflo Ltd. - http:// www. Cyflogic .com/).

Mitochondrial membrane potential

For the assessment of mitochondrial membrane potential, cells were seeded and exposed following the steps explained above. After trypsinization, the cells were counted and centrifuged at 500 x g for 5 min. The cells were subsequently re-suspended in 500 mL of diluted MitoCapture^{TM} solution. Samples were incubated at 37°C in a 5% CO_2 incubator for 20 min. After centrifugation, cells were re-suspended in 1 mL of the pre-warmed Incubation Buffer and analyzed by flow cytometry.

Aggresome detection assay

The ubiquitin-proteasome system plays an important role in the controlled degradation of intracellular proteins in eukaryotic cells. [8, 9, 16] Autophagy is responsible for the elimination and recycling of cytoplasmic components such as misfolded proteins that are modified to enter the proteosomal pathway for degradation. [8] The aggresome detection kit composes of the ProteoStat aggresome detection reagent, Hoechst 33342 that stains the nucleus, Proteasome Inhibitor and 10 x Assay Buffer. Cells treated with 5 µM Proteasome Inhibitor (MG-132) served as positive control. After exposure to C19 and DMSO as vehicle control, the cells were trypsinized and the cell suspension was collected. Centrifugation of the cell suspension for 5 min was followed by 2 rinsing steps with 2 mL 1 x Assay Buffer. After centrifugation, the cell pellet was re-suspended in the remaining buffer and 2 mL of 4% formaldehyde was added in a drop-wise manner while slowly stirring. The samples were left at room temperature for 30 min. Subsequently, samples were centrifuged at 800 x g the supernatant was discarded, re-suspended in the remaining volume of supernatant and 2 mL of 1 x Assay Buffer was added and the cells were centrifuged at 800 x g for 15 min. Two mL of permeabilizing solution was added drop-wise while stirring and samples were subsequently incubated on ice for 30 min. Cells were collected by centrifugation at 800 x g for 15 min and washed. After another centrifugation step, cells were re-suspended in 500 µL of diluted ProteoStat Aggresome Red Detection Reagent. Samples were protected from light, incubated at room temperature for 30 min and analyzed in the FL3 channel of a flow cytometer. Aggresome activity factor (AAF) value was calculated by obtaining the mean fluorescence intensity (MFI) values for treated and untreated samples using the formula:

$$AAF = 100 \times (MFI_{treated} - MFI_{control})/MFI_{treated}$$

According to the supplier's instructions, an AAF value greater than 25 is indicative of autophagy.

Autophagy detection: Rabbit polyclonal anti-LC3B conjugated to DyLight 488

The autophagy protein LC3, is the only recognized mammalian protein identified that stably associates with the autophagosome membranes. LC3-I is cytosolic and LC3-II is membrane bound and enriched in the autophagic vacuole fraction. The detection of the conversion of LC3-I to LC3-II is a useful and sensitive marker for identifying autophagy

in mammalian cells.[17] LC3B antibody allowed for autophagy detection. Exponentially growing MCF-7 cells were seeded at 500 000 cells per 25cm^2 flask. After 24 h attachment the medium was discarded and cells were exposed to 0.18 μM C19 and incubated for 24 h. Cells were washed with cold PBS and pelleted. Cells were fixed with 3 ml 0.01% formaldehyde in PBS for 10 min at 4°C. Cells were centrifuged and resuspended in 200 μl PBS, followed by 1ml ice-cold methanol (-20°C) for 15 min at 4°C. Afterwards cells were washed twice with cold PBS. Cells were stained with the 0.5 ml antibody cocktail (0.05% Triton, 1% BSA, 40 μg/ml propidium iodide and 0.5 μg/ml conjugated rabbit polyclonal anti-LC3B antibody) prepared in PBS for 2 h at 4°C. Cells were washed trice with PBS/0.05% Triton x-100/1% BSA and analyzed with flow cytometry. Data from at least 10 000 cells were analyzed by means of Cyflogic version 1.2.1 software (Pertu Therho, Turko, Finland).

Statistical analysis of data

Data obtained from at least three biological repeats for mitochondrial membrane potential, cell cycle analysis, caspase 7 and 8, LC3 and aggresome quantification were obtained. Only one set of representative data are shown. Quantitative data were statistically analyzed for significance using the analysis of variance (ANOVA)-single factor model followed by a student's *t*-test. Means are represented in bar charts with T-bars referring to standard deviations. *P*-values of <0.05 were regarded as statistically significant. Qualitative experiments were repeated at least twice where data were obtained from PlasDIC, haematoxylin and eosin staining and fluorescent microscopy.

Results

MORPHOLOGY

Triple staining

Fluorescent triple staining was conducted to examine the cells for possible hallmarks of apoptosis and autophagy after a 24 h exposure to 0.18 μM C19. Acridine orange stains autophagic vacuoles and lysosomes with an increase in green fluorescence. Hoechst 33342 penetrates cell membranes of viable cells and cells undergoing apoptosis and the stained

nuclei will emit a blue fluorescence. Propidium iodide stains the nuclei of cells that have lost their membrane's integrity due to oncotic or necrotic processes with a red fluorescence. An increase in green fluorescence was observed in the C19-treated sample (Figure 2D) when compared to the controls (Figures 2A and 2B). Hypercondensed chromatin was observed in the actinomycin-D treated cells (Figure 2C) and cell density was compromised in the C19-treated sample (Figure 2D). No red fluorescence was observed indicating that cell membranes were not disrupted.
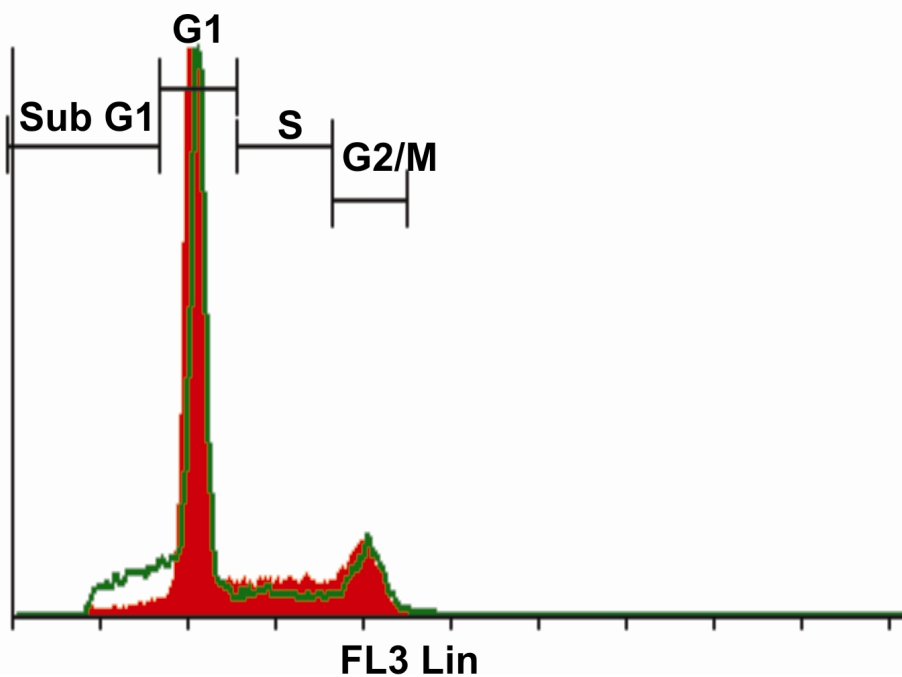
Figure 2. Triple-stained MCF 7 cells propagated in growth medium (A), exposed to DMSO (B) actinomycin D (C) and C19 (D). C19-treated cells revealed an intense green fluorescence indicating increased lysosomal activity. Actinomycin D-treated cells exhibit features of late stages of apoptosis including hypercondensed chromatin and the presence of apoptotic bodies (magnification 400x).

Polarization-optical differential interference contrast

PlasDIC was used to visualize the morphological effects of 0.18 μM of C19 on MCF-7. MCF-7-treated cells revealed an increase in the number of cells blocked in metaphase, as well as shrunken cells (Figure 3D). The density of the treated sample was compromised when compared to the density of controls (Figure 3A-D). Apoptotic bodies were observed in both C19-treated and actinomycin-D treated cells (Figure 3C-D).
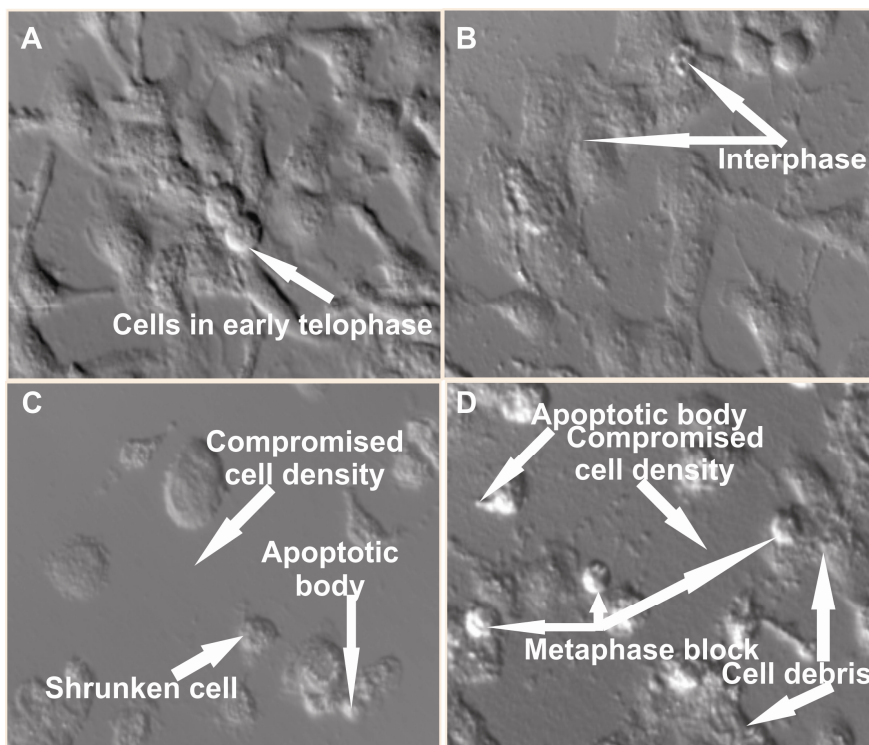
Figure 3. Polarization-optical differential interference contrast images of MCF-7 cells propagated in medium only (A), starved cells (B), actinomycin D-treated cells (C) and 0.18 μM C19-treated cells (D) after a 24 h exposure time. MCF-7 treated with C19 showed cells blocked in metaphase while cells present in telophase and interphase were observed in cells propagated in medium only (magnification 400x).
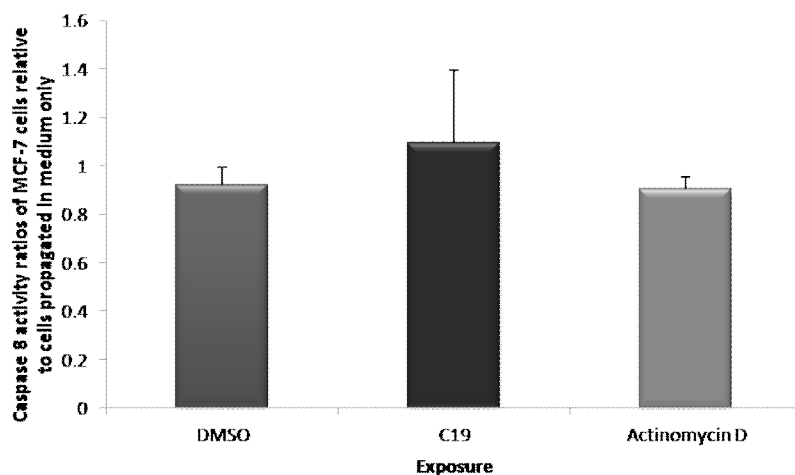

Figure 4. Light microscopy displayed MCF-7 cells propagated in medium only (A), vehicle control cells (B) and 0.18 μM C19-treated cells (C) after a 24 h exposure time. MCF-7 exposed to C19 showed mitotic block while cells in metaphase, anaphase and interphase were observed in cells propagated in medium only and vehicle-control sample (magnification 400x). Quantitative analysis provided in (D) showed an increase in the number of cells in metaphase in the C19-treated cells when compared to the vehicle-control sample.

Haematoxylin and eosin staining

Haematoxylin and eosin staining revealed hypercondensed chromatin, apoptotic bodies, metaphase block and compromised density in the C19-treated MCF-7 cells when compared to the vehicle-treated cells (Figure 4).

SPECTROPHOTOMETRY

Caspase 7 and 8 activation assay

The purpose of this study was to determine whether $0.18\mu M$ of C19 increases caspase 7 and 8 activity in MCF-7 cells after 24 h of exposure. The ratio of caspase 7 and 8 activity was measured with reference to cells propagated in medium only. Positive controls for both caspase 7 and 8 were included in the experimental design (data not shown). The C19-treated sample showed an increase in caspase 8 activity after a 24 h exposure time, however, this increase was not statistically significant (Figure 5). A statistically significant increase in caspase 7 activity in C19-treated cells compared to vehicle treated cells was observed.
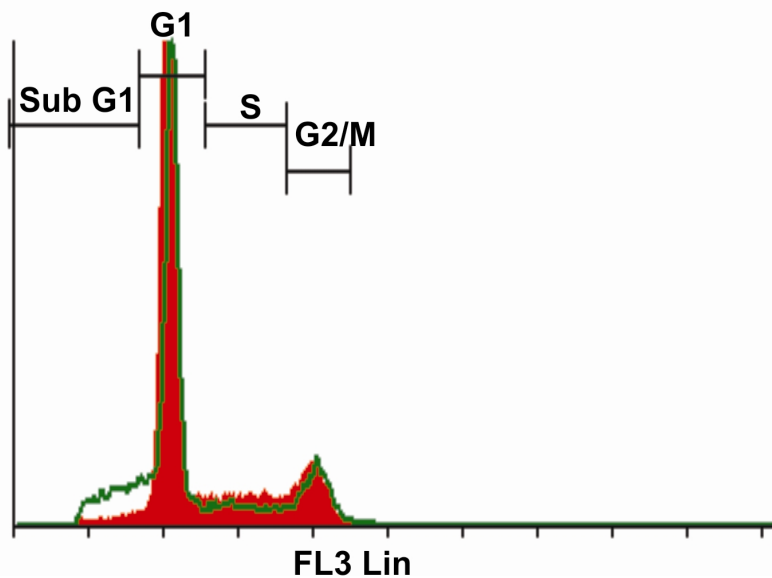

Figure 5. Caspase 7 and 8 activity ratios of C19-treated cells compared to cells in medium only after 24 h of exposure. Caspase 8 activity was not statistically significantly increased in the C19-treated cells when compared to cells propagated in medium only. A statistically significant increase in caspase 7 activity in C19-treated cells compared to vehicle treated cells was observed. An asterisk (*) indicates a *P*-value <0.05 when compared to the vehicle control.

FLOW CYTOMETERY

Cell cycle analysis

Flow cytometric analysis revealed the increased amount of cells in sub-G_1 phase in the C19-treated sample in comparison with the vehicle control sample (Figure 6). Table 1 indicates the percentage of the C19-treated and vehicle control samples in the different phases.

Table 1: Cell cycle progression of vehicle-treated MCF-7 and C19-exposed MCF-7 cells

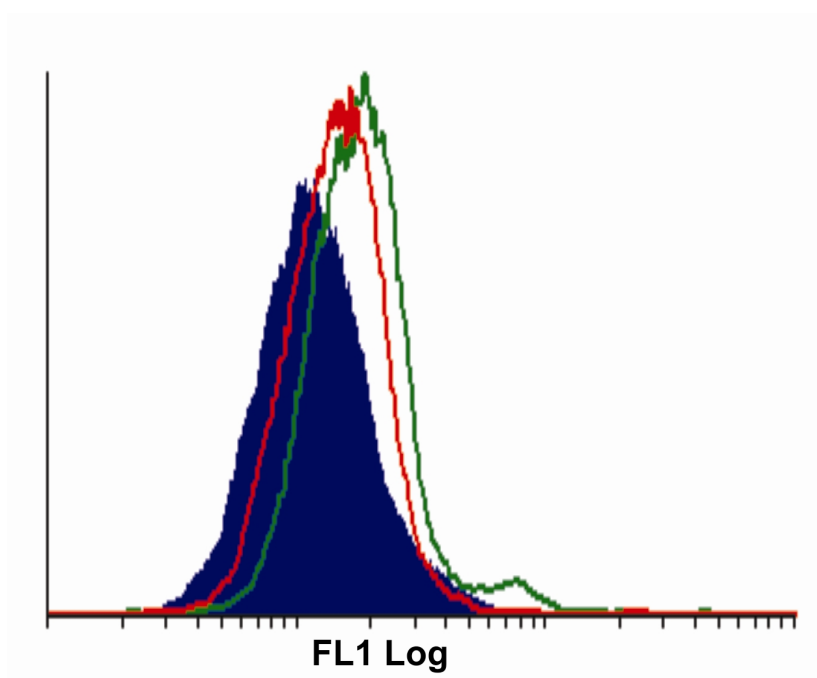|	Vehicle control sample (%)	C19-treated sample (%)
Sub G_1	2.51	12.8
G_1	70.24	62.26
S	13.56	10.11
G_2	13.19	14.42

FL1 Log

Figure 6. Flow cytometric analysis of cell cycle progression showed an increased sub-G_1 in C19-exposed cells when compared to the vehicle control sample. The vehicle control sample is indicated as the red solid filled area, with C19-treated sample represented as the green solid line.

Mitochondrial membrane potential.

Analysis of the membrane potential showed an increase in the number of cells with a reduced membrane potential in the C19-treated sample when compared to the vehicle control sample

(Figure 7). This increase in reduced membrane potential was represented by a shift to the right on the histograms. There was a two-fold increase in the number of cells with reduced membrane potential in C19-treated sample when compared to the vehicle-control (table 2). The results are expressed as FL1 Log histograms.

Table 2: Analysis of reduction in mitochondrial membrane potential

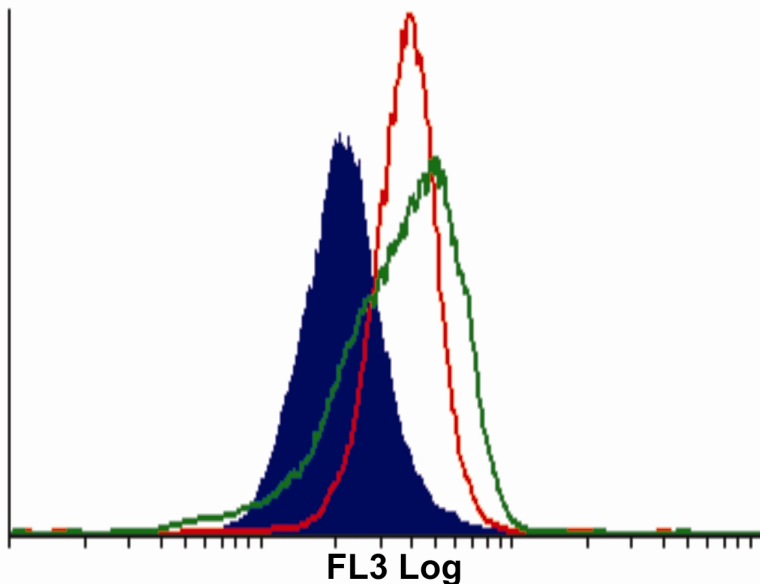| MCF-7	Number of cells with reduced membrane potential
DMSO	7.41
Tamoxifen	16.46
C19	19.27

FL3 Log

Figure 7. Flow cytometry revealed an increase in the number of cells with reduced membrane potential in the C19-treated cells in comparison to the vehicle treated sample. The vehicle control sample was symbolized by the blue histogram, actinomycin D-treated sample is represented by the red solid line and the C19-treated sample is shown as the green solid line.

Aggresome detection assay

The assessment of aggresome formation by flow cytometry showed an increase in the number of aggresomes formed in the C19-treated sample when compared to the vehicle control sample (Figure 8). This was represented by a shift to the right. The ratio of aggresomes formed was obtained by calculation of the aggresome activity factor (AAF) using the mean

fluorescence intensity (MFI) of treated and control samples, as indicated in table 3. Results are expressed as FL3 Log histograms.

Table 3: Aggresome formation detection (mean fluorescence intensity (MFI))

MCF-7	MFI
DMSO	7.28
Tamoxifen	15.1
C 19	15.0

AAF: 100x (15.0- 7.28)/15.0= 51%

If the AAF value is greater than 25%, this indicates the formation of aggresomes.
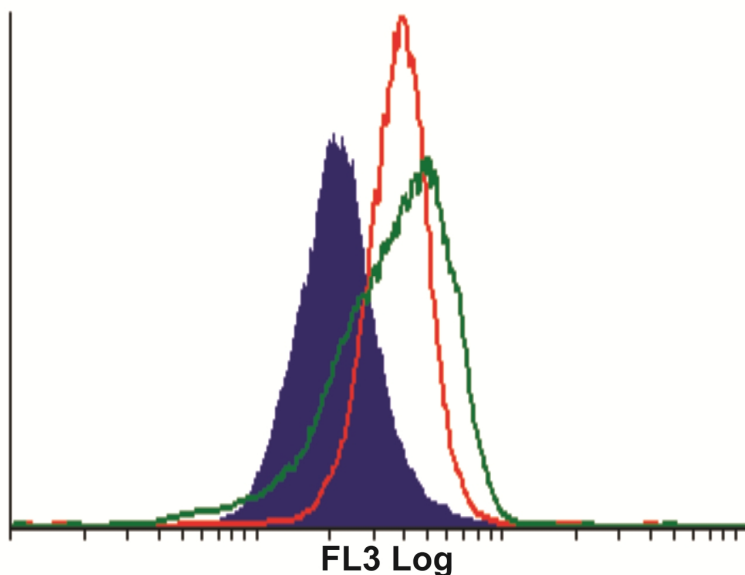

FL3 Log

Figure 8. Flow cytometry revealed a shift to the right in the Actinomycin-D (solid red line) and C19-treated (green solid line) samples when compared to the vehicle control sample (filled area). This shows an increase in aggresome formation.

Autophagy detection: Rabbit polyclonal anti-LC3B conjugated to DyLight 488

A conjugated rabbit polyclonal anti-LC3 antibody using flow cytometry was employed for the detection of autophagy. The latter demonstrated the accumulation of LC3 in 38% of the C19-treated cells when compared to 31% of the vehicle-treated cells (Figure 9).
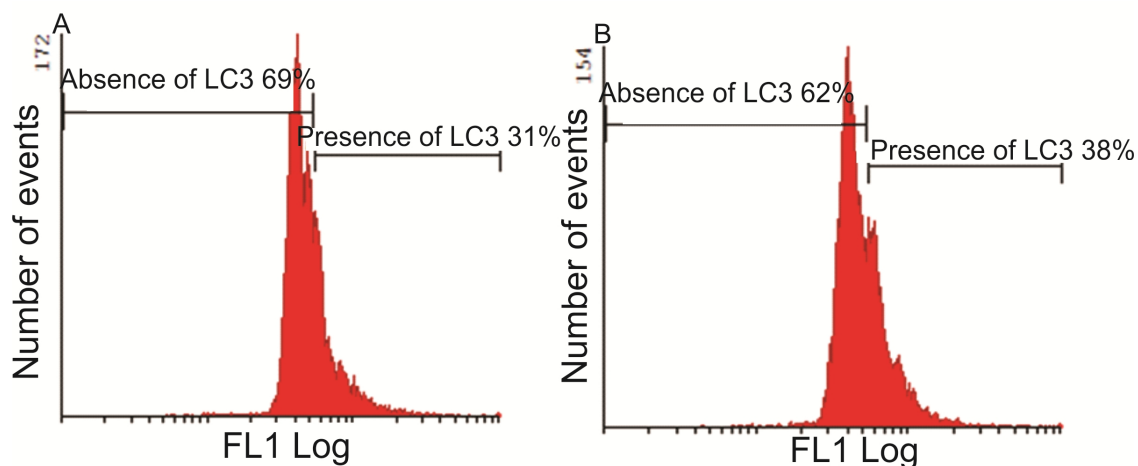
Figure 9. Flow cytometrical investigation employing the conjugated anti-LC3B antibody for the detection of autophagy in vehicle-treated cells (A) and C19-treated cells (B) revealed that 38% of C19-treated MCF-7 cells were present in autophagy when compared to vehicle-treated cells.

Discussion

Previous research conducted in our laboratory revealed that 0.18 μM C19 inhibited MCF-7 cell growth by 50% after 24 h of exposure. [4] Similar results were obtained by Vorster *et al*. (2010) in MCF-12A cells after treatment with 2ME2 and 2-MeOE2bisMATE. [7] Subsequently, and in order to provide more insight into C19's antiproliferative effects, the influence of 0.18 μM C19 was determined on cell morphology, caspase activity, cell cycle progression, mitochondrial membrane potential and aggresome formation after an exposure time of 24 h in MCF-7 cells. Another preliminary study showed that treatment of MDA-MB-435 cells with 2ME2 inhibited growth in a time- and dose-dependent manner. [3] Hallmarks of apoptosis, namely cells blocked in metaphase, hypercondensed chromatin, apoptotic bodies, as well as a compromised cell density were observed within the MCF-7 cell line exposed to 0.18 μM of C19. An intense green fluorescence was also observed in the C19-treated sample indicating increased lysosomal activity and possible induction of autophagy.

Caspase 8 activity was not statistically increased in the C19-treated samples. Caspase 8 is an initiator in the extrinsic pathway of apoptosis [18,19] culminating in the activation of executioner caspases 3, 6, and 7. [20] Caspase 7 activity was increased significantly in the C19-treated cells. Caspase 7 is one of the downstream executioner caspases along with caspases 3 and 6. [20] Effector caspases are responsible for the morphological changes associated with apoptotic cell death namely shrunken cells, apoptotic bodies formation and subsequent reduced cell

density.[21] Another study revealed an increase in the activation of caspases 3, 7 and 9 in MDA-MB-435 cells after treatment with 2 μM of 2ME2 for 12, 24, and 36 h in a time-dependent manner. [3] Azab *et al.* (2009) showed that the combination of doxorubicin (DOX), a prominent chemotherapeutic agent for the treatment of breast cancer, and 2ME2 resulted in an increase in caspase 3 activity by up to 27-fold in a dose-dependent fashion, suggesting that the activation of effector caspases may be involved in the 2ME2 chemosensitizing effect to DOX. [22]

DNA content was measured as an indication of cells in various stages of the cells cycle to evaluate C19's effect on cell cycle progression. MCF-7 cells displayed a sub-G_1 fraction indicative of apoptosis. Apoptosis was confirmed by PlasDIC by means of decreased cell density, cell debris and the presence of apoptotic bodies. Flow cytometry demonstrated reduction of mitochondrial membrane potential in the treated cells. Stander *et al.* (2011) also showed an increase in the number of cells in the G_2/M phase after 24 h exposure and an increase in the number of cell in the sub-G_1 fraction after 48 h in the MDA-MB-231 cells treated with newly synthesized estrone analogues namely compounds 2-ethyl-3-O-sulfamoyl-estra-1,3,5(10),15-tetraen-3-ol-17-one and 2-ethyl-estra-17 methylbenzenesulfenohydrazide at different concentrations. [4] Concurrently, Van Zijl *et al.* (2008) confirmed that 2ME2-treated MCF-7 cells caused a metaphase block, membrane blebbing, apoptotic body formation, and disruption of spindle formation. These researchers revealed that 10^{-6} M 2ME2 reduced cell growth by 84% in MCF-7 cells and only by 44% in MCF-12A cells, implying that the tumorigenic cell line is more sensitive to 2ME2 treatment than the normal cell line. [23]

The mitochondrial membrane potential of cells was evaluated to suggest induction of apoptosis via the intrinsic pathway. The disruption of the mitochondrial membrane is one of the earliest events that occur after induction of apoptosis. The induction of apoptosis is accompanied by the mitochondrial permeability transition which is characterized by the drop in the electrochemical gradient across the mitochondrial membrane due to the formation of pores in the membrane. The formation of pores is initiated by the activation of proapoptotic members of the Bcl-2 family (Bax, Bid, Bak, Bad proteins). [24] After disruption of the mitochondrial membrane, cytochrome *c*, normally found in the inner mitochondrial membrane and involved in the electron transport chain, [25] is released in the cytosol and the activity of effector caspase increases. [24,26-28] The intrinsic pathway of apoptosis is mediated

via the mitochondria. An increase in Bcl-2 expression and a decrease in Bax expression may foresee the response to chemotherapy in breast cancer cells [29] and the Bcl-2: Bax ratio predicts the cell fate. [24] An increase in the number of cells with reduced membrane potential was observed in the C19-treated MCF-7 cells. Fukui *et al.* (2009) observed similar results after exposure of MDA-MB-435 cells to 2ME2 for 42 h. [3] Reduction in mitochondrial membrane potential was observed. In addition it was demonstrated that pretreatment of cells with an inhibitor of ERK or p38 enhanced 2ME2-induced reduction in mitochondrial membrane potential. [3] The assessment of aggresome formation suggests cell death by autophagy. C19- and tamoxifen-treated cells a showed a shift to the right. This shift suggests that there is an increase in the number of aggresomes formed. A two-fold increase in the AAF value was observed in the C19-treated MCF-7 cells.

As previously mentioned, fluorescence microscopy revealed lysosomal staining, thus suggesting the novel discovery of autophagy induction by C19. Conjugated rabbit polyclonal anti-LC3B antibody employing flow cytometry verified the induction of autophagy by C19 in the tumorigenic MCF-7 cell line. Autophagy is a process by which the cell's own components are broken down to maintain a balance of synthesis and degradation in the metabolism of all eukaryotic cells when the cells are undergoing stress.[30] Azab *et al* (2009) demonstrated that 2ME2 induced autophagy in human glioblastoma-astrocytoma epithelial-like cell line (U87), human cervical adenocarcinoma cells (HeLa) and transformed human embryonic kidney cells (HEK293).[22]

In conclusion, C19 treatment of MCF-7 cells resulted in apoptosis which was observed by the presence of apoptotic bodies, shrunken cells, disruption of the mitochondrial membrane potential and caspase 7 activation. An increase in aggresomes formation and an increase in lysosomal activity in the C19-treated sample suggest occurrence of autophagy. LC3 accumulation in the C19-treated cells confirmed cell death by autophagy. This is the first time that an increase in aggresome formation is observed in C19-treated MCF-7 cells and the exact role of the increased aggresome formation and cell death remains to be determined. This novel compound induced cell death by both apoptosis and autophagy in the breast adenocarcinoma MCF-7 cell line. Cross-talk between autophagy and apoptosis occurs at many levels since both pathways share mediators. [20, 31, 32] Future studies are underway to further investigate the signal transduction pathway of C19 in MCF-7 cells and to identify cross-talk targets affected by C19 in both apoptosis and autophagy *in vitro*.

Conflict of interest

None known.

Acknowledgements

References

1. Dranitsaris G, Truter I, Lubbe, MS, Amir E, Evan W. Advances in cancer therapeutics and present access to new drugs. *Pharmacoeconomics* 2011; **29**: 213-224.

2. Hulka BS, Moorman PG. Breast cancer: hormones and other risk factors. *Maturitas* 2008; **61**: 203-213.

3. Fukui M, Zhu BT. Mechanism of 2-methoxyestradiol-induced apoptosis and growth arrest in human breast cancer cells. *Mol Carcinog* 2009; **48**: 66-78.

4. Stander BA, Joubert F, Joubert AM. Docking, synthesis, and *in vitro* evaluation of antimitotic estrone analogues. *ChemBiol Drug Des* 2011; **77**: 173-181.

5. Visagie MH, Joubert AM. The *in vitro* effects of 2-methoxyestradiol-bis-sulphamate on cell numbers, membrane integrity and cell morphology, and the possible induction of apoptosis and Autophagy in a non-tumorigenic breast epithelial cell line. *Cell Mol Biol Lett* 2010; **15**: 565-581.

6. Joubert AM, Marais S, Maritz C. Influence of 2-methoxyestradiol on MCF-7 cells: An improved differential interference contrasting technique and Bcl-2 and Bax protein expression levels. *Biocell* 2009; **33**: 67-70.

7. Vorster CJJ, Joubert AM. *In vitro* effects of 2-methoxyestradiol-bis-sulphamate on the non-tumorigenic MCF-12A cell line. *Cell Biochem Funct* 2010; **28**: 412-419.

8. Bursch W, Karwan A, Mayer M, Dornetshuber J, Fröhwein U, Schulte-Hermann R, *et al*. Cell death and Autophagy: Cytokines, drugs, and nutritional factors. *Toxicology* 2008; **254**: 147-157.

9. Hung CC, Davison EJ, Robinson PA, Ardley HC. The aggravating role of the ubiquitin-proteasome system in neurodegenerative disease. *Biochem Soc Trans* 2006; **34**: 743-745.

10. Snoeks TJ, Mol IM, Que I, Kaijzel EL, Lowik CW. 2-methoxyestradiol analogue ENMD-1198 reduces breast cancer-induced osteolysis and tumor burden both *in vitro* and *in vivo*. *Mol Cancer Ther* 2011; **10**: 874-882.

11. Zhou Q, Gustafson D, Nallapareddy S, Diab S, Leong S, et al. A phase I dose-escalation, safety and pharmacokinetic study of the 2-methoxyestradiol analog ENMD-1198 administered orally to patients with advanced cancer. *Invest New Drugs* 2011; **29**: 340-346.

12. Pasquier E, Sinnappan S, Munoz MA, Kavallaris M. ENMD-1198, a new analogue of 2-methoxyestradiol, displays both antiangiogenic and vascular-disrupting properties. *Mol Cancer Ther* 2010; **9**: 1408-1418.

13. Moser C, Lang SA, Mori A, Hellerbrand C, Schlitt HJ, et al. ENMD-1198, a novel tubulin-binding agent reduces HIF-1 alpha and STAT3 activity in human hepatocellular carcinoma (HCC) cells, and inhibits growth and vascularization *in vivo*. *BMC Cancer* 2008; **8**: 206.

14. LaVallee TM, Burke PA, Swartz GM, Hamel E, Agoston GE, et al. Significant antitumor activity in vivo following treatment with the microtubule agent ENMD-1198. *Mol Cancer Ther* 2008; **7**: 1472-1482.

15. Agoston GE, Shah JH, Suwandi L, Hanson AD, Zhan X, et al. Synthesis, antiproliferative, and pharmacokinetics properties of 3- and 17-double-modified analogs of 2-methoxyestradiol . *Bioorg Med Chem Lett* 2009; **19**: 6241-6244.

16. Levine B, Kroemer G. Autophagy in the pathogenesis of disease. *Cell* 2008; **132**: 27-42.

17. Kanzawa T, Germano IM, Komata T, Ito H, Kondo, Kondo S. Role of autophagy in temozolomide-induced cytotoxicity for malignant glioma cells. *Cell Death Differ* 2004; **11**:448-457.

18. Singh R, Pervin S, Chaudhuri G. Caspase-8-mediated BID cleavage and release of mitochondrial cytochrome c during N-hydroxy-L-arginine-induced apoptosis in MDA-MB-468 Cells. *J Biol Chem* 2002; **277**: 37630-37636.

19. Kang SJ, Kim BM, Lee YJ, Hong SH, Chung HW. Titanium dioxide nanoparticles induce apoptosis through the JNK/p38-caspase-8-Bid pathway in phytohemagglutinin-stimulated human lymphocytes. *Biochem Biophys Res Commun* 2009; **386**: 682-687.

20. Jin Z, Li Y, Pitti R, Lawrence D, Pham VC, Lill JR, et al. Cullin3-based polyubiquitination and p62-dependent aggregation of caspase-8 mediate extrinsic apoptosis signaling. *Cell* 2009; **137**:721-35.

21. Cicek M, Iwaniec UT, Goblirsch MJ, et al. 2-Methoxyestradiol Suppresses Osteolytic Breast Cancer Tumor Progression *In vivo*. *Cancer Res* 2007; **67**: 10106-10111.

22. Azab SS, Salama SA, Abdel-Naim AB, Khalifa, AE, El-Demerdash E, Al-Hendy A. 2-Methoxyestradiol and multidrug resistance: can 2-methoxyestradiol chemosensitize resistant breast cancer cells? *Breast Cancer Res Treat* 2009; **113**: 9-19.

23. Van Zijl C, Lottering ML, Steffens F, Joubert AM. *In vitro* effects of 2-methoxyestradiol on MCF-12A and MCF-7 cell growth, morphology, and mitotic spindle formation. *Cell Biochem Funct* 2008; **26**: 632-642.

24. Nehra R, Riggins RB, Shajahan AN, Zwart A, Crawford AC, Clarke R. BCL 2 and CASP 8 regulation by NF-kB differentially affect mitochondrial function and cell fate in antiestrogen-sensitive and-resistant breast cancer cells. *FASEB J* 2010; **24**: 2040-2055.

25. Foster PA, Ho TY, Newman SP, Kasprzyk PG, Leese MP, Potter BVL, Reed MJ, et al. 2-MeOEbisMATE and 2-EtE2bisMATE induce cell cycle arrest and apoptosis in breast cancer xenografts as shown by a novel ex vivo technique. *Breast Cancer Res Treat* 2008; **111**: 251-260.

26. Narita M, Shimizu S, Ito T, Chittenden T, Lutz RJ, Matsuda H, et al. Bax interacts with the permeability transition pore to induce permeability transition and cytochrome c release in isolated mitochondria. *Proc Natl Acad Sci USA* 1998; **95**: 14681-14686.

27. Luo X, Budihardjo I, Zou H, Slaughter C, Wang X. Bid, a Bcl2 interacting protein, mediates cytochrome c release from mitochondria in response to activation of cell surface death receptors. *Cell* 1998; **94**:481-490.

28. Basanez G, Nechushtan A, Drozhinin O, Chanturiya A, Choe E, Tutt S, et al. Bax, but not Bcl-xL, decreases the lifetime of planar phospholipid bilayer membranes at subnanomolar concentrations. *Proc Natl Acad Sci USA* 1999; **96**: 5492-5497.

29. Reed JC. Regulation of apoptosis by bcl-2 family proteins and its role in cancer and chemoresistance. *Curr Opin Oncol* 1995; **7**: 541-546.

30. Tsujimo Y, Shimizu S. Another way to die: autophagic programmed cell death. *Cell Death Differ* 2005; **12**:1528-1534.

31. Maiuri MC, Zalckvar E, Kimchi A, Kroemer G. Self-eating and self-killing: crosstalk between autophagy and apoptosis. *Nat Rev Mol Cell Biol* 2007; **8**:741-52.

32. Yang ZJ, Chee CE, Huang S, Sinicrope FA. The role of Autophagy in Cancer: Therapeutic Implications. *Mol Cancer Ther* 2011; **10**: 1533-1541.